

# Study of SiO<sub>2</sub>-PbO-CdO-Ga<sub>2</sub>O<sub>3</sub> glass system for mid-infrared optical elements

Xavier Forestier<sup>a, b</sup>, Jarosław Cimek<sup>a, c</sup>, Ireneusz Kujawa<sup>a</sup>, Rafał Kasztelanic<sup>a, c</sup>, Dariusz Pysz<sup>a</sup>, Krzysztof Orliński<sup>a</sup>, Ryszard Stępień<sup>a</sup>, Ryszard Buczyński<sup>a, c</sup>

<sup>a</sup> Institute of Electronic Materials Technology, Wolczynska 133, 01-919 Warsaw, Poland

<sup>b</sup> Warsaw University of Technology, Faculty of Physics, Koszykowa 75, 00-662 Warsaw, Poland

<sup>c</sup> University of Warsaw, Faculty of Physics, Pasteura 5, 02-093 Warsaw, Poland

## Abstract:

Glasses based on SiO<sub>2</sub>-PbO-CdO-Ga<sub>2</sub>O<sub>3</sub> system have been studied for the first time for fabrication of mid-infrared optical elements. Gallium oxide concentration was gradually increased, replacing silicon dioxide, for different cadmium and lead oxide content. The thermal and optical properties were investigated for different compositions. It was observed that the thermal stability, refractive index, and the transmission in the infrared range increased with increase of gallium and lead concentrations. The most thermally stable glass composition was selected for fabrication of optical elements such as optical fibers. We also successfully fabricated mid-infrared lenses by hot embossing for potential application in compact gas detectors.

**Keywords:** soft glass, glass synthesis, infrared optics, hot embossing, optical fibers.

## Highlights:

- Thermal and optical properties of SiO<sub>2</sub>-PbO-CdO-Ga<sub>2</sub>O<sub>3</sub> glass system were investigated.
- Substitution of silicon dioxide with gallium oxide decreases glass susceptibility to crystallization without significant change in refractive index.
- The most thermally stable glass composition of 28SiO<sub>2</sub>-45PbO-15CdO-12Ga<sub>2</sub>O<sub>3</sub> is suitable for the fabrication of lenses by the hot embossing method and for the fabrication of optical fibers.

## 1. Introduction:

Recently, development of optical components dedicated for mid-infrared wavelengths has attracted considerable interest due to market demands. Indeed, mid-infrared wavelength range, generally defined between 2 μm to 15 μm, finds many applications in environmental monitoring, food safety, biomedical sensing or in the defence industry. Polymer materials cannot be used in this range due to very high attenuation. Glasses for infrared optics like optical fibers or lenses require the use of materials with appropriate composition to ensure high transmission in this range of wavelengths, as well as good mechanical and physicochemical properties including good chemical durability. Moreover the thermal processes involved in fiber drawing using the stack and draw method [1] and in lenses molding by the hot embossing method [2-3] require the glass to be stable regarding crystallization over a wide range of temperatures. The optical and thermo-physical properties of the main type of glasses used in infrared optics are presented in Table 1.

Table 1 Main properties of the families of glass used in infrared optic

		n at 1.55 $\mu$ m	$n_2 \times 10^{20}$ (m <sup>2</sup> /W)	Transmission ( $\mu$ m)	CTE $\alpha_{20/300}$ (10 <sup>-7</sup> .K <sup>-1</sup> )	T <sub>g</sub> (°C)	Ref
Silicates	silica	1.44	2.73	0.2 to 2.7	5.9	~1200	[4]
	borosilicate (BK7)	1.50	3.60	0.3 to 2.5	73	~498	[5]
	lead silicate (SF57)	1.80	41	0.41 to 4.5	92	~414	
	HMOG with silica	1.8-2.2	30-100	0.4 to 5.5	70 to 100	400 to 500	[6] [7]
Fluorides	ZBLAN	1.51	3.3	0.3 to 8	200	~265	[8]
Heavy metal oxides glass		1.8-2.2	30-100	0.4 to 7	80 to 120	230 to 400	[9]
Chalcogenides	As <sub>2</sub> S <sub>3</sub>	2.45	400-600	0.62 to 11.53	230	~185	[10]
	As <sub>2</sub> Se <sub>3</sub>	2.81	1400-3000	0.85 to 17.5	250	~178	
	Te <sub>20</sub> As <sub>40</sub> Se <sub>40</sub>	2.9	>2000	1.23 to 18.52	230	~140	

Silica glasses are widely used in optics for telecommunication applications considering their excellent transmission and their low attenuation losses in the visible and the near infrared. Silica-based fibers can also be doped with transition metals or rare earth ions for optical amplifier application, doped with erbium or neodymium for example [11-13]. However, their increasing absorption above 2  $\mu$ m excludes applications in the mid-infrared.

Soft glasses and particularly heavy metals oxides, chalcogenides and fluoride glasses present the advantage to have an extended transmission in the infrared and have higher linear and nonlinear refractive indices, which makes them particularly interesting for the development of optical components in the infrared. They also present the advantage to have lower processing temperatures.

Fluoride glasses, with their extremely broad transmission from ultraviolet to the mid-infrared, up to 8  $\mu$ m, have a linear and nonlinear refractive indices similar to silicates. Moreover, their high rare-earth solubility and their low attenuation allow fiber lasers application [14-15] or generation of supercontinuum with ultrashort high power pulses [16]. On the other hand, this family of glasses has poor chemical durability if compared to heavy metal oxides ones.

Chalcogenide glasses offer a large transmission window in the infrared, high linear and nonlinear refractive indices as well as low phonon energy, which makes them excellent host materials for amplifier and laser applications [17], despite their rather low rare earth solubility [18]. Their unique properties of high transmission window also makes them appropriate for application in IR optics such as thermal imaging [19], metrology [20], military defense systems or medicine [21]. Sulfur and selenium based glasses have a transparency up to 10  $\mu$ m and 16  $\mu$ m respectively [22]. Tellurium based glasses, on the other hand, can exhibit a multiphonon cut-off wavelength up to over 24  $\mu$ m due to Te higher atomic weight [23]. However, due to the strong metallic character of tellurium, they have a tendency to crystallize during thermal processing.

On the other hand, heavy metal oxides glasses (HMOG) have a limited transmission in the mid-IR up to 6-7  $\mu$ m and a refractive index ranging from 1.8 to over 2.2 but have the advantage to have a good transparency starting in the visible and overall better mechanical properties [24]. They offer a good compromise between optical properties, cost and are relatively easy to synthesize. Lead gallium glass system, lacking typical glass formers, exhibits a low thermal stability. Previous studies have shown that the introduction of SiO<sub>2</sub> in lead-gallium glasses increases the crystallization resistance, due to the stabilizing role of [SiO<sub>4</sub>] tetrahedra in the glass network, while keeping the transmission over 4.5  $\mu$ m [25]. In addition, gallium oxide dramatically improves the thermal stability of heavy metal oxides glasses against devitrification [26]. Incorporating Ga<sub>2</sub>O<sub>3</sub> into glass compositions additionally increases the linear and nonlinear index of refraction [27-30]. Lead oxide

is known to increase the refractive index due to its high optical density and large molecular weight. It also decreases the viscosity and the characteristic temperature due to the creation of non-bridging oxygen in silicate glasses, below 30% content. Above 30%, PbO starts to act as a glass former and enter the glass network with PbO<sub>x</sub> polyhedron, further decreasing the transition temperature [31-32]. Such multicomponent system allows to easily tune the thermomechanical and optical properties by modifying the concentration of the components [33].

The goal of the present work is to develop glasses with the appropriate rheological properties for the fabrication of optical elements such as micro-lenses and fiber optics with high transmittance in mid-infrared. We have chosen to study the glass system containing SiO<sub>2</sub>-PbO-CdO-Ga<sub>2</sub>O<sub>3</sub> (named SPCG) that was not considered before. In this aim, we studied in the proposed SiO<sub>2</sub>-PbO-CdO-Ga<sub>2</sub>O<sub>3</sub> system, the impact of the substitution of silica by gallium oxide on the thermal and optical properties for different lead oxide and cadmium oxide contents. We consider the most stable glasses against crystallization for the fabrication of optical fibers by the stack and draw method as well as lenses by the hot embossing method.

## 2. Synthesis of SiO<sub>2</sub>-PbO-CdO-Ga<sub>2</sub>O<sub>3</sub> glass composition

The glasses were prepared by the conventional melt-quenching technique using analytical grade substrates SiO<sub>2</sub>, CdO, Ga<sub>2</sub>O<sub>3</sub>, PbO and As<sub>2</sub>O<sub>3</sub> as fining agent [32]. Fining agents are used to obtain glasses with high optical quality. As<sub>2</sub>O<sub>3</sub> is used in combination with oxidant, lead nitrates in this case, to convert As<sub>2</sub>O<sub>3</sub> to As<sub>2</sub>O<sub>5</sub>. During the fining, at higher temperature, pentavalent arsenic will release O<sub>2</sub> in the melt, promoting gas removal from the molten glass, increasing the homogeneity. The substrates were weighed and ground to obtain homogenous powder followed by drying at 150°C for twelve hours. Batches were finally melted in alumina crucibles for 2 hours, at a temperature ranging from 1000°C to 1100°C, depending on the composition, in a resistance furnace. Melts have been mechanically stirred several times to obtain a good homogeneity and have then been poured into a preheated graphite mold before being annealed, from 460 degrees to the room temperature, at a rate of 0.5°C/min. In order to investigate the influence of the composition on the properties and to develop thermally stable glasses for mid-infrared optical elements, 3 series of glasses have been synthesized: series D, with the general composition (40-x)SiO<sub>2</sub>-35PbO-25CdO-xGa<sub>2</sub>O<sub>3</sub>, series B, (40-x)SiO<sub>2</sub>-40PbO-20CdO-xGa<sub>2</sub>O<sub>3</sub> and series C, (40-x)SiO<sub>2</sub>-45PbO-15CdO-xGa<sub>2</sub>O<sub>3</sub>, with x=0, 3, 6, 9, 12 and 15 %mol. The chemical compositions are presented in Table 2.

Table 2: Chemical composition (in mol%) of SPCG B, C and D series of glasses

Composition of SPCG glasses (mol%)																		
Oxide	(40-x)SiO <sub>2</sub> -40PbO-20CdO-xGa <sub>2</sub> O <sub>3</sub>						(40-x)SiO <sub>2</sub> -45PbO-15CdO-xGa <sub>2</sub> O <sub>3</sub>						(40-x)SiO <sub>2</sub> -35PbO-25CdO-xGa <sub>2</sub> O <sub>3</sub>					
	0B	1B	2B	3B	4B	5B	0C	1C	2C	3C	4C	5C	0D	1D	2D	3D	4D	5D
SiO <sub>2</sub>	40	37	34	31	28	25	40	37	34	31	28	25	40	37	34	31	28	25
PbO	40	40	40	40	40	40	45	45	45	45	45	45	35	35	35	35	35	35
CdO	20	20	20	20	20	20	15	15	15	15	15	15	25	25	25	25	25	25
Ga <sub>2</sub> O <sub>3</sub>	-	3	6	9	12	15	-	3	6	9	12	15	-	3	6	9	12	15

## 3. Measurement procedure of SiO<sub>2</sub>-PbO-CdO-Ga<sub>2</sub>O<sub>3</sub> glass

The viscosities were determined by a combination of hot stage microscopy (HSM), dilatometry ( $\eta = 10^{11}$  P) and differential scanning calorimetry ( $\eta = 10^{13.4}$  P). HSM consists of a cubic sample (dimension 4 x 4 x 4 mm) heated in a furnace with a 10°C/min heating rate and observed with an objective. The viscosities have been determined depending on the evolution of the shape of the samples. When the corners of the cube round out, the viscosity  $\eta = 10^9$  P. As the temperature increases, the sample goes from a spherical shape at  $T_{sph}$  ( $\eta = 10^6$  P) to a hemispherical shape at  $T_{hs}$  ( $\eta = 10^4$  P) to finally spread at lower viscosity ( $\eta = 10^2$  P) [34-35]. Characteristic temperatures ( $T_c$ ,  $T_{hs}$ ,  $T_{sph}$ ,  $T_{spr}$ ) were determined by the observation of the sample shape through the objective. Several measurements were performed and show an accuracy of  $\pm 5^\circ\text{C}$ .

The linear coefficients of thermal expansions along with the dilatometric softening temperatures ( $\eta = 10^{11}$  P),  $T_{dsp}$ , have been determined with a Bahr Thermoanalyse GmbH Dil801 dilatometer with 5°C/min heating rate, under air. The accuracy of the linear expansion coefficient is  $\pm 0.03 \cdot 10^{-6} \text{ K}^{-1}$ , whereas the accuracy on the temperature measurement is  $\pm 1^\circ\text{C}$ . Measurements were performed on rods with the dimension 4 x 4 x 30 mm.

Glass transition temperatures  $T_g$ , as well as the crystallization onset temperature  $T_x$ , were determined by differential scanning calorimetry (DSC) using STA 449 F1 Jupiter (NETZSCH) equipped with a platinum furnace. Samples of 60 mg were heated in alumina crucibles with 10 K/min heating rate under the flow of a mixture comprising argon (72 ml/min) and oxygen (18 ml/min), in the range 30-800°C. The thermal stability of the glasses can be evaluated by the difference  $\Delta T = T_x - T_g$  introduced by Dietzel [36]. A glass is stable enough for fiber drawing if  $\Delta T$  is above 100°C and if it has a good crystallisation resistance over a wide range of temperature. Indeed the various heat treatments involved in the production of optical elements can lead to the devitrification of the glass.

Additional crystallization tests have been carried out with an isothermal heat treatment, 20°C higher than the sphere creation temperature  $T_{sph}$  ( $\log \eta \sim 4-5$  P), for 2 hours and then cooled down to room temperature. Samples were then observed under microscope with a polarizing attachment to detect eventual crystals growth due to the heat treatment.

The density of the glasses has been determined at room temperature by the conventional Archimedes method, using distilled water as immersion liquid, at room temperature. From the density and the average molar weight of the glass, the molar volume has been calculated using the following formula:

$$V_m = \sum_{i=1}^n x_i \cdot M_i / \rho \quad (\text{cm}^3 \cdot \text{mol}^{-1}) \quad (1)$$

Where  $x_i$  is the molar fraction and  $M_i$  is the molecular weight of the  $i^{\text{th}}$  component and  $\rho$  the glass density in  $\text{g} \cdot \text{cm}^{-3}$ .

Glass transmittance measurements have been conducted with a spectrophotometer Bruker IFS 113V from 2  $\mu\text{m}$  to 6  $\mu\text{m}$  with 2 mm thickness polished samples.

The group refractive index has been measured using the Michelson interferometry technique with a Thorlabs CCS220 spectrometer from 200 nm to 1000 nm and an Avantes AvaSpec-NIR256-1.7 spectrometer from 1  $\mu\text{m}$  to 1.7  $\mu\text{m}$ . The systematic error calculated for the group refractive index measurement is  $\pm 4 \cdot 10^{-4}$ . The phase refractive indices (2) were determined from the Sellmeier coefficients, retrieved by fitting the first derivative of the Sellmeier equation (3) to the measured group refractive indices [37].

$$n(\lambda) = \sqrt{1 + \frac{B_1 \lambda^2}{\lambda^2 - C_1} + \frac{B_2 \lambda^2}{\lambda^2 - C_2} + \frac{B_3 \lambda^2}{\lambda^2 - C_3}} \quad (2)$$

Where  $n$  is the phase refractive index at wavelength  $\lambda$  in  $\mu\text{m}$ ,  $B_1, B_2, B_3$  and  $C_1, C_2, C_3$  are constants determined by the fitting process.

$$N(\lambda) = n(\lambda) - \lambda \cdot \frac{dn(\lambda)}{d\lambda} = n(\lambda) + \frac{\lambda^2}{n(\lambda)} \cdot \sum_{i=1}^n \frac{B_i \cdot C_i}{(\lambda^2 - C_i)^2} \quad (3)$$

Where  $N(\lambda)$  is the group refractive index,  $n(\lambda)$  the phase refractive index,  $\lambda$  the wavelength in  $\mu\text{m}$ ,  $B_i$  and  $C_i$  are constants determined by the fitting process.

The optical dispersion of the glasses have been evaluated from their respective Abbe V-number calculated from:

$$v_D = \frac{n_D - 1}{n_F - n_C} \quad (5)$$

With  $n_D$ ,  $n_F$ , and  $n_C$  respectively the indices of refraction for the sodium D line (589.3 nm), the hydrogen F line (486.1 nm) and the hydrogen C line (656.3 nm).

The material dispersion of the bulk glasses has then been calculated from the second derivative of the Sellmeier equation such as:

$$D(\lambda) = -\frac{\lambda}{c} \cdot \frac{dn^2}{d^2\lambda} \quad (6)$$

## 4. Results and discussion

### 4.1 DSC measurements

The DSC measurement results for the 3 series of glass are presented Figure 1. The transformation temperature  $T_g$ , crystallization onset temperature  $T_x$  and the difference  $\Delta T = T_x - T_g$  are summarized in Table 3.

Table 3 Characteristic temperatures of SPCG glasses determined by DSC

Serie B	$T_g$ (°C)	$T_x$ (°C)	$\Delta T = T_x - T_g$	Serie C	$T_g$ (°C)	$T_x$ (°C)	$\Delta T = T_x - T_g$	Serie D	$T_g$ (°C)	$T_x$ (°C)	$\Delta T = T_x - T_g$
SPCG0B	455.3	613.5	158.2	SPCG0C	439.5	575	135.5	SPCG0D	459.5	581.7	122.2
SPCG1B	454.0	691.4	237.4	SPCG1C	443.5	596	152.5	SPCG1D	467.8	613.2	145.4
SPCG2B	460.3	660.9	200.6	SPCG2C	451.7	649.7	198.0	SPCG2D	474.0	617.9	143.9
SPCG3B	465.6	670.7	205.1	SPCG3C	460	652.7	192.7	SPCG3D	478.8	619	140.2
SPCG4B	468.1	670.5	202.4	SPCG4C	460.8	654.2	193.4	SPCG4D	480.3	677.5	197.2
SPCG5B	468.0	655.3	187.3	SPCG5C	464.5	652	187.5	SPCG5D	480.8	679.2	198.4

\*Accuracy of the measurement was evaluated comparing the melting point of different pure metals in the range of measurement (100 - 900°C). The accuracy is  $\pm 0.3^\circ\text{C}$  due to varying heat transfer conditions such as the position of the crucible in the heating chamber, the mass of the sample and the heating rate.

Glasses with 0 % and 3 % gallium in all series present multiple sharp crystallization peaks, characteristic of a high tendency to crystallize and point to the presence of multiple crystalline phases. The most stable glasses with 6 % to 15 %  $\text{Ga}_2\text{O}_3$  are characterized by a very low intensity crystallization peak and a good

nonisothermal crystallization resistance with  $\Delta T$  ranging from 150 K to 205 K. Additional endothermic reactions of unknown nature are observed in the  $\Delta T$  region. The thermal stability of all series increases with the substitution of  $\text{SiO}_2$  with  $\text{Ga}_2\text{O}_3$ , as well as the glass transition temperature (Fig 2), ranging from  $439^\circ\text{C}$  to  $480^\circ\text{C}$ . We observe also that replacing cadmium oxide with lead oxide leads to a diminution of the characteristics temperatures. Indeed, an increase of  $\text{PbO}$  concentration instead of  $\text{CdO}$ , decreases the glass transition temperature.

The additional isothermal crystallization test confirmed that SPCG 3, 4 and 5 of each series are the most suitable to make optical elements and have been selected for further tests for hot embossing and fiber drawing applications. In these cases, no crystallites were observed under the polarizing microscope after 2 hours of heat treatment at  $T_{\text{sph}} + 20 \text{ K}$ , in contrast with SPCG 0, 1 and 2 of each series, for which complete or partial crystallization was observed. We conclude that increasing  $\text{Ga}_2\text{O}_3$  content with simultaneous reduction of  $\text{SiO}_2$  leads to a large augmentation of the thermal stability of the glass, as shown in Table 3.

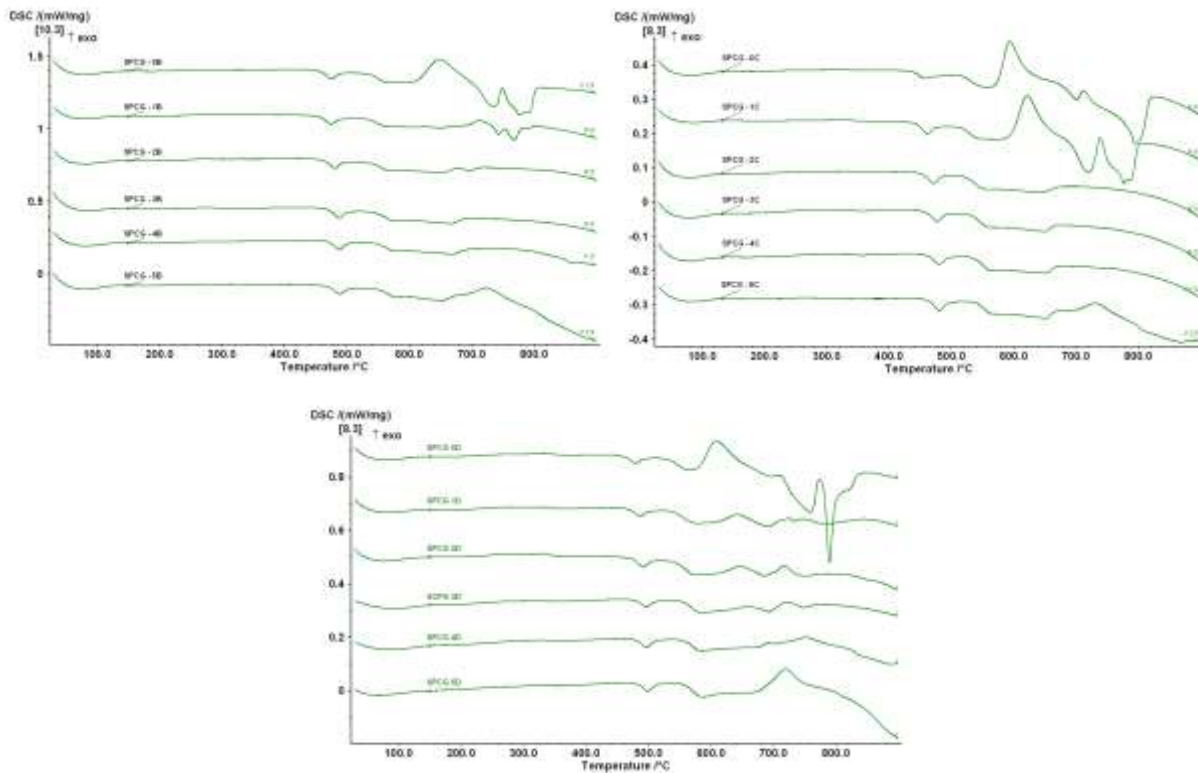


Figure 1 DSC curves for SPCG B series (left), SPCG C series (right) glasses and SPCG D series (down).

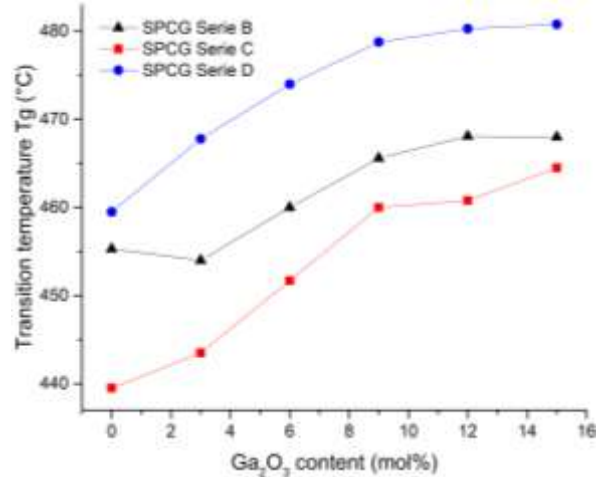
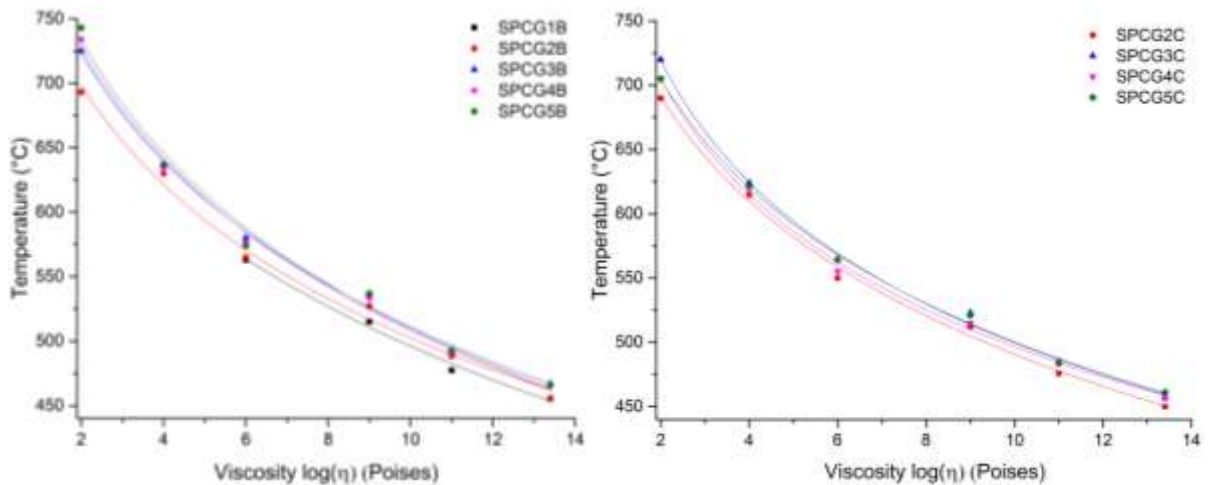


Figure 2 Evolution of the glass transition temperature with the gallium oxide content.

#### 4.2 Viscosity measurements

The evolution of the temperature dependence of the viscosity is presented in Figure 3. The glasses containing 0 and 3% Ga<sub>2</sub>O<sub>3</sub> concentration have shown a high tendency to devitrify, therefore, the viscosities at high temperature could not be obtained by hot stage microscopy due to the crystallization of the sample between the curvature and the sphere temperatures. Further increase of Ga<sub>2</sub>O<sub>3</sub> concentration leads to a monotonic augmentation of the viscosity. Substituting PbO with CdO leads to an increase of the viscosity as well. Series D (35%PbO/25%CdO) presents the highest viscosities among all series of glass whereas series C (45%PbO/15%CdO) has the lowest. The viscosity increases with an increasing Ga<sub>2</sub>O<sub>3</sub> and CdO content, which is consistent with previous studies [38] showing that an increasing lead oxide molar percentage decreases the viscosity of lead silicate glasses. The measured viscosity characteristics of glasses shows that they are technologically short, which makes fabrication of fibers by the stack and draw technique delicate. If we consider the glass processing viscosity between  $\eta=10^4$  and  $10^8$  Poises for the production of optical elements, the working temperature range is comprised between 525 °C and 615 °C (Fig.3). Due to the different nature of the measurements involved (as explained section 3), the viscosity curves, logarithmically fitted with the Levenberg-Marquardt algorithm, is added as a guide for the eyes to get the general trend of the different glass compositions.



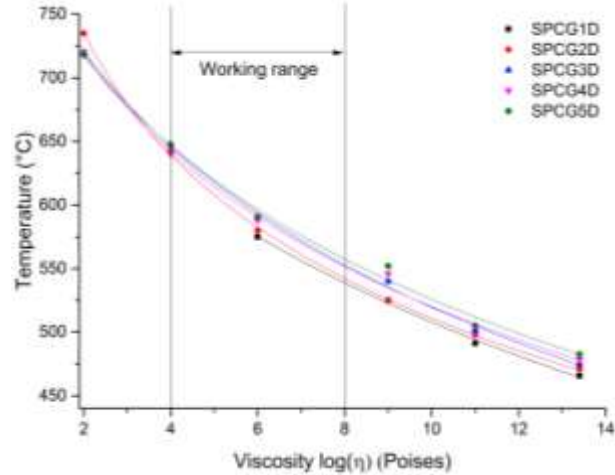


Figure 3 Viscosity-Temperature relationship of SPCG glasses for B, C and D series

### 4.3 Density and molar volume

The density increases with the increase of gallium oxide content (Fig.4). This is related to the substitution of lighter atoms of Si with heavier atoms of Ga in the network which leads to increase the average molecular weight of the glass. The density anomaly observed at 9% content of  $Ga_2O_3$  disappears, if we calculate the molar volume. Indeed, the molar volume is more sensitive to structural changes than is density because it is normalized for atomic weights of different glass components. We observe an augmentation of the molar volume with an increasing  $Ga_2O_3$  molar percentage (Fig. 5). In general, density and molar volume vary in opposite way, this atypical behavior between density and molar volume has been previously reported also for other glass systems [39-40]. In the present case, this may be attributed to the molecular weight of the glass increasing more rapidly than the density. The density of series B is much higher than the 2 other series leading to the lowest molar volume among the 3 series, which may point to a structural change at 40% PbO.

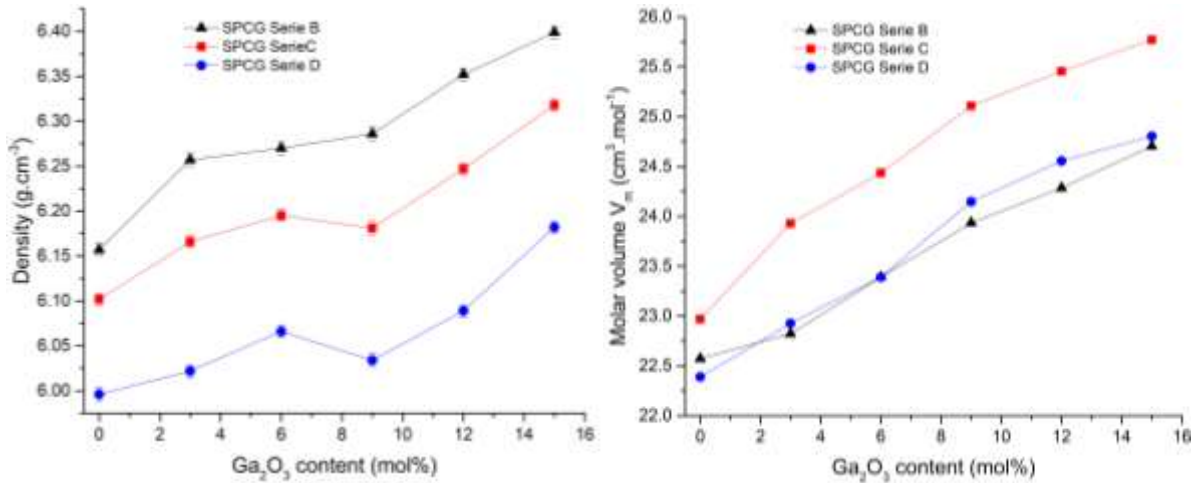


Figure 4 Evolution of the density (left) and molar volume (right) of SPCG glasses with  $Ga_2O_3$  content.



Table 4 Properties of SPCG glasses series

Glass	CTE $\alpha_{300}^{20}$ ( $10^{-6}K^{-1}$ ) $\pm 0.03$	$T_{dsp}$ ( $^{\circ}C$ ) $\pm 1$	Characteristics temperatures in Hot Stage Microscopy ( $^{\circ}C$ ) $\pm 5^{\circ}C$				Cristallization	Density $\rho$ ( $g/cm^3$ ) $\pm 0.007$	Molar Volume ( $cm^3/mol$ ) $\pm 7.10^{-4}$	Abbe Number	Refractive index $n_d$
			Curvature	Sphere	Hemisphere	Spreading					
			$T_c$	$T_s$	$T_{hs}$	$T_{spr}$					
SPCG0B	9.15	477.8	510	Xsed	Xsed	Xsed	yes	6.157	22.573	-	-
SPCG1B	8.95	477.3	515	563	Xsed	Xsed	yes	6.257	22.822	20.0	1.945
SPCG2B	8.53	488.4	527	565	630	693	yes	6.27	23.389	18.5	1.957
SPCG3B	8.26	491.4	537	580	637	725	no	6.286	23.934	19.7	1.975
SPCG4B	8.15	491	533	576	634	734	no	6.352	24.285	19.4	1.982
SPCG5B	8.2	493	537	574	637	743	no	6.399	24.705	18.6	1.991
SPCG0C	9.06	462.4	Xsed	Xsed	Xsed	Xsed	yes	6.141	22.969	20.5	1.965
SPCG1C	8.73	466.2	500	Xsed	Xsed	Xsed	yes	6.166	23.929	19.6	1.970
SPCG2C	8.59	475.8	512	550	615	690	yes	6.195	24.435	-	-
SPCG3C	8.4	484.8	523	565	624	720	yes	6.181	25.108	19.1	1.980
SPCG4C	8.26	484.4	515	555	620	705	no	6.247	25.455	18.6	1.992
SPCG5C	8.42	483.6	521	564	622	705	no	6.318	25.771	17.8	1.998
SPCG0D	9.27	483.6	545	Xsed	Xsed	Xsed	yes	5.996	22.389	21.4	1.940
SPCG1D	8.54	491.2	525	575	Xsed	Xsed	yes	6.022	22.926	21.2	1.944
SPCG2D	8.26	497.8	530	581	642	730	yes	6.066	23.391	20.4	1.948
SPCG3D	8.18	501.7	540	590	648	720	no	6.034	24.147	20.2	1.956
SPCG4D	8.51	498.3	546	588	640	720	no	6.089	24.556	19.5	1.970
SPCG5D	8.37	505.1	552	591	647	718	no	6.182	24.804	19.3	1.980

#### 4.4 Optical Properties

The transmission measurements are presented in Fig. 5. All series of developed glasses show a broad spectral window in the mid-infrared, up to 5.0  $\mu m$ . Increasing the gallium oxide content leads to shifting the multiphonon edge towards longer wavelengths, whereas the substitution of lead oxide by cadmium oxide lets the transmission in infrared almost unchanged. The intensity of the characteristic absorption peak related to the presence of hydroxyl ions  $OH^-$ , as well as the transmission cut-off wavelength, increase with the gallium content. We also noticed that the absorption peak intensity around 3  $\mu m$  decreases with the substitution of  $PbO$  with  $CdO$ . This shows that lead oxide tends to retain more water than cadmium oxide. The strong water absorption is mostly due to the synthesis without protective atmosphere as well as the water contained in the initial components.

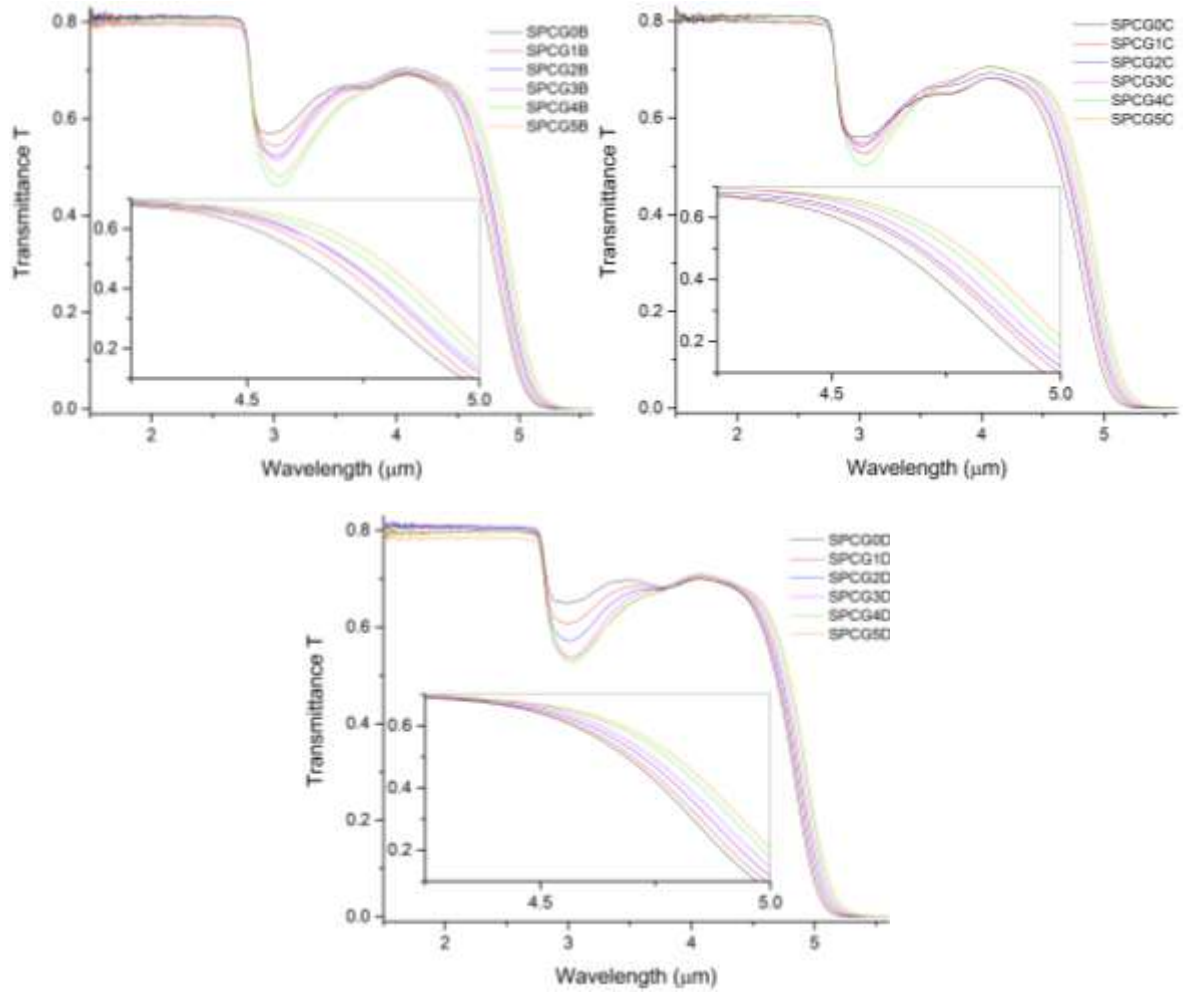


Figure 5 Transmittance of SPCG glasses in the range 2 to 6  $\mu\text{m}$ .

The refractive indices have been calculated from the group refractive index, measured with a Michelson interferometer as discussed section 3, from 500 to 1700 nm. The sodium D line (589.3 nm) has been used to compare the glasses and are ranging from 1.940 to 1.998 among the 3 series. The substitution of silica by gallium, as well as an increasing lead oxide content, lead to an augmentation of the refractive index. As shown in Figure 6, the highest refractive index is obtained for Series C with 45 %mol PbO ( $n_D=1.998$ ) and the lowest for series D with 35 %mol PbO ( $n_D=1.940$ ). The material dispersion  $D$ , calculated from the second derivative of the Sellmeier equation (Eq. 6), follows the exact same trend (Fig. 7). The evolution of the reciprocal relative dispersion, or Abbe V-number, with the composition is summarized in Table 4. The optical dispersion is high for all glasses and increases with the gallium percentage. The Sellmeier coefficients of the glasses are summarized in the annex 1.

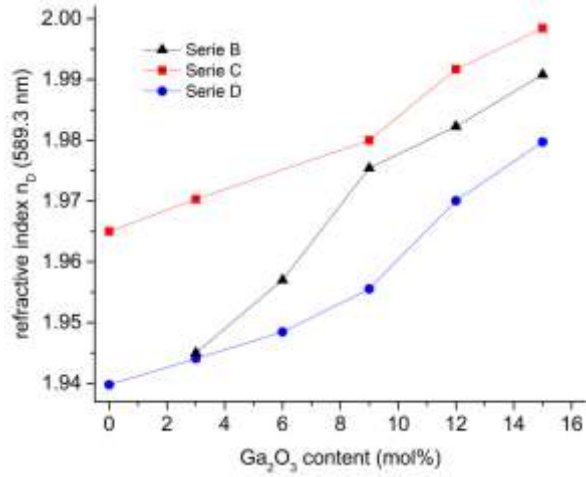


Figure 6 Evolution of the refractive index at 589.3 nm as a function of  $Ga_2O_3$  content.

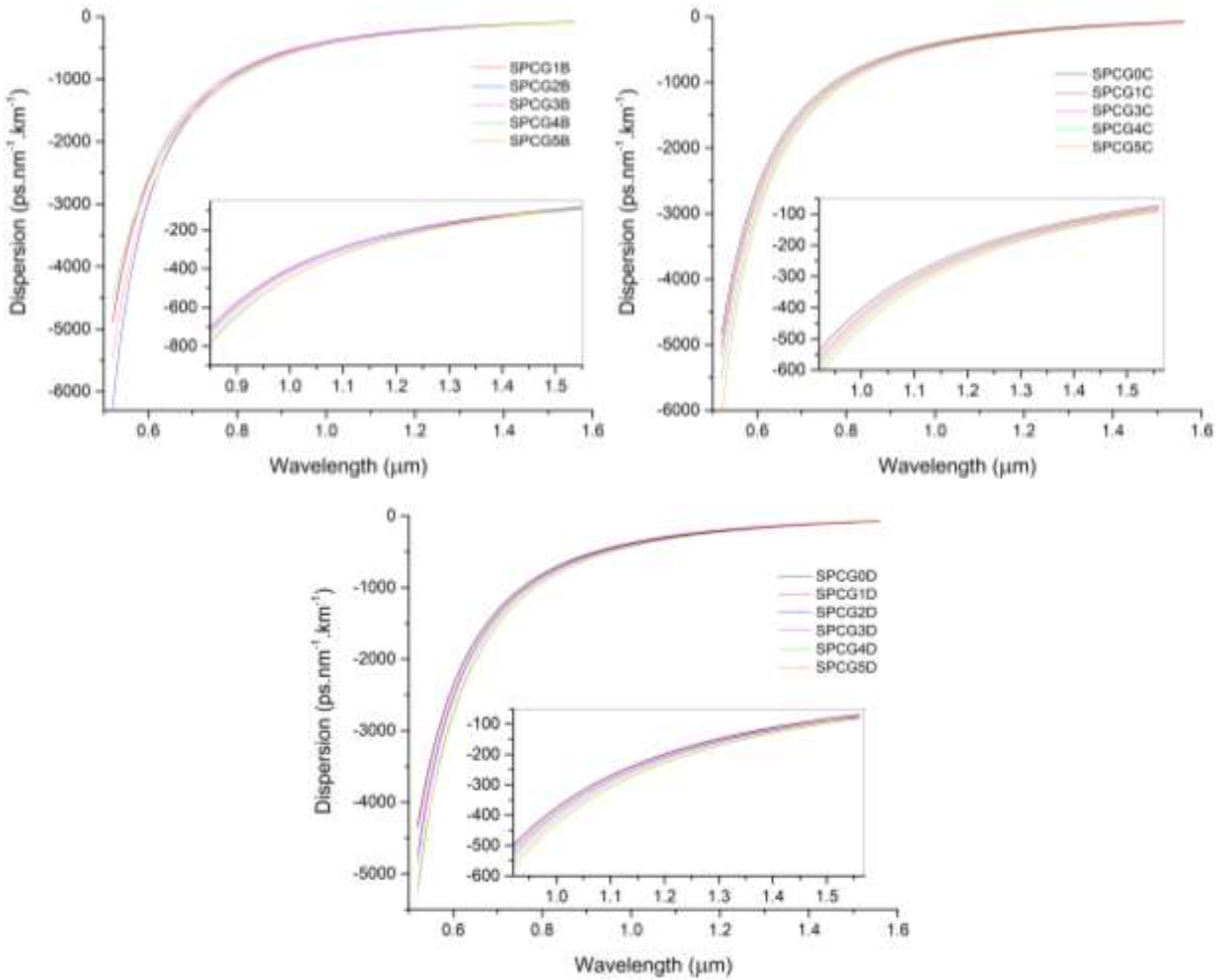


Figure 7 Dispersion parameter  $D$  as function of the wavelength for the 3 series of glasses.

## 5. Verification of use of selected $\text{PbO-SiO}_2\text{-CdO-Ga}_2\text{O}_3$ glasses for fiber and micro-optic development

Hot embossing process presents the advantage to be one of the lowest-cost methods for the fabrication of optical elements. It consists in an upper and lower stamps heated to the desired temperature [41]. When the optimal temperature of the glass is attained, the desired shape is finally transferred by pressure of the molding stamps. One of the most important steps to make lenses by the hot embossing technique is the choice of the mold material. Indeed, the coefficient of thermal expansion (CTE) of the glass must match the chosen mold to avoid cracking during the process. In addition, the glass must not adhere to the mold and has to be crystallization resistant. We have selected brass and cemented carbide for their very close CTE. These materials were successfully used as molds for hot embossing with heavy metal oxide glasses previously [42]. We've selected the glasses with -the largest  $\Delta T$  criterion (SPCG 3, 4, 5 of each series) which resisted to the isothermal crystallisation test (according to section 4.1) and have conducted preliminary embossing tests. SPCG4C glass was synthesized at increased volume without any changes of the optical and thermal properties which proves a good repeatability of the experiments. Different molding parameters have been tested until the obtention of a lens. Such parameter, beside the choice of the mold, are the molding temperature, the force applied and the molding duration. Based on the quality of the lens and the eventual presence of cracks or irregularities of the surface of the different lenses developed from the 3 series, we have finally chosen SPCG4C glass for its good thermal stability and its capacity to form good quality lenses. Indeed, other glasses could not be molded properly or showed cracks. The optimal parameters used for this composition were a temperature of  $602^\circ\text{C}$ , the pressure force of the piston was 194 N for a duration of 10 seconds.

The quality of the lens has been evaluated with a white light interferometer Veeco Wyko NT2000. The images of the surfaces are shown in Figure 8a and 8b. Figure 8c shows the profile of the center of the surface of the lens of the convex side, whereas figure 8d shows the flat side of the lens. The curvature of the lens is too pronounced to measure beyond the central part of the lens using a white light interferometer. The average roughness calculated from the profile is around  $0.05\ \mu\text{m}$  for the spherical surface whereas the roughness of the flat surface is  $0.088\ \mu\text{m}$  which is acceptable for applications in the mid-infrared. The standard error of this measurement  $\text{SE}=0.02\ \mu\text{m}$ .

The focal length of the lens has been determined using a fiber coupled laser source from Thorlabs at  $1550\ \text{nm}$  with a power set at  $0.05\ \text{mW}$  and an infrared camera (Fig.9). The focus in our experiment is at a distance of  $15.2\ \text{mm}$  from the last surface of the lens. The Back Focal Length,  $\text{BFL} = 11.71\ \text{mm}$  which allows to state that the Effective Focal Length,  $\text{EFL} = 11.72\ \text{mm}$ . Errors in the horizontal and vertical direction are  $\pm 1\ \mu\text{m}$ , and  $\pm 0.5\ \mu\text{m}$  respectively.

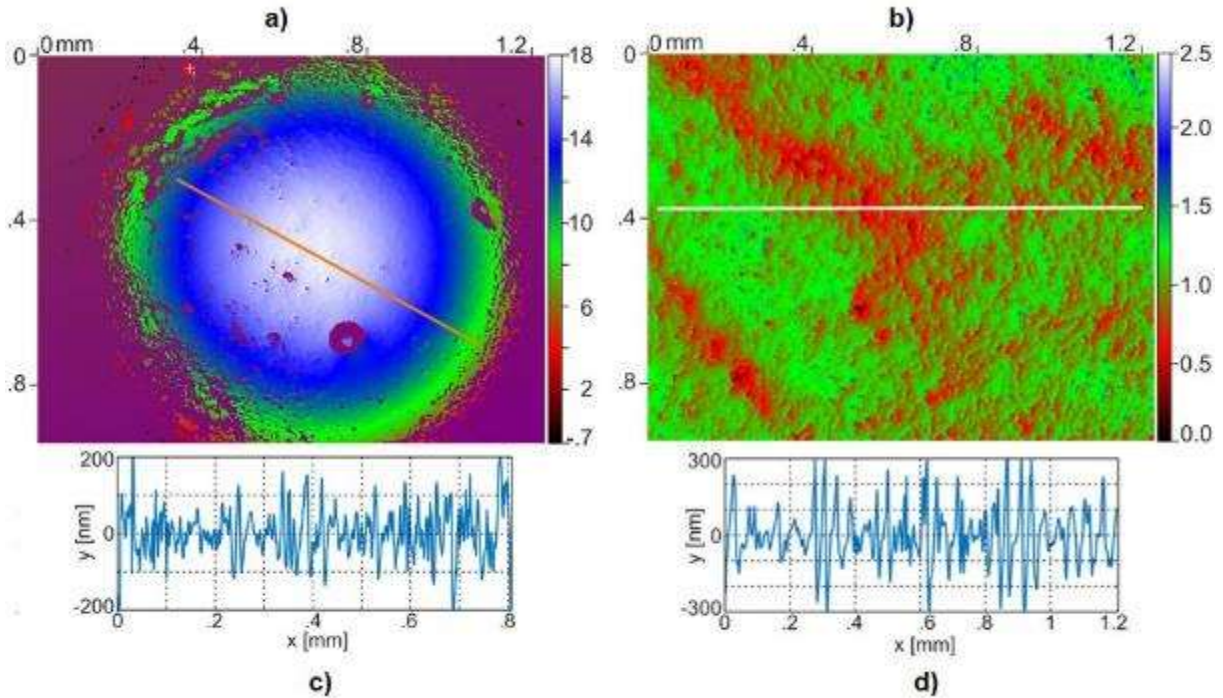


Figure 8: Surface quality measurements of the developed lens obtained using a white light interferometry method. a) and b) are respectively the scan of the spherical surface and of the flat side of the lens, while c) and d) are the respective surface roughness profiles along the line represented on the scans

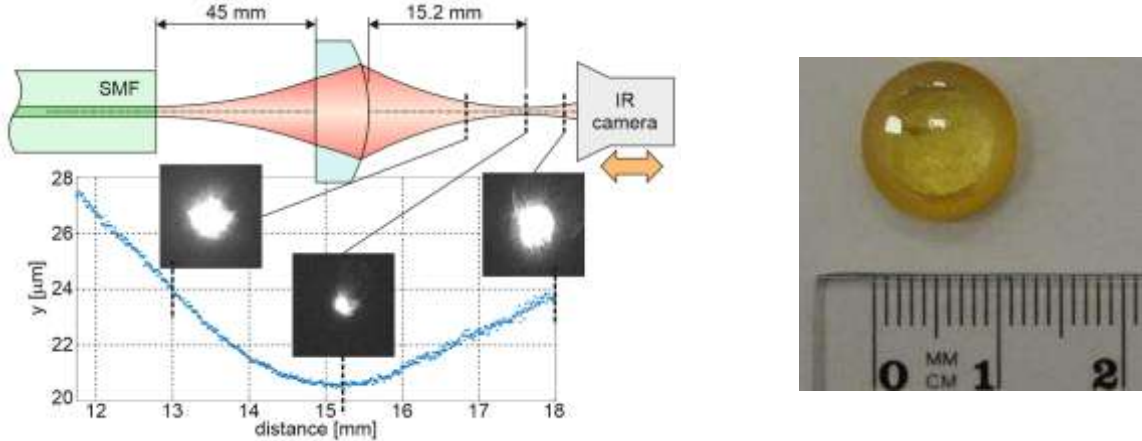


Figure 9 (left) Experimental setup for the measurement of the effective focal length of the lens, (right) fabricated lens based on SPCG4C glass

We also verified the possibility to use the selected glass (SPCG4C) for the development of optical fibers by a classic fiber drawing technique considering its high thermal stability. The preform is fed into a furnace that heat it up to decrease its viscosity, in order to be drawn. Glass fiber is pulled by capstan while the preform is constantly fed into the furnace with constant speed. During the drawing process, fiber is coated by polymer (acrylate) which is UV cured. For this purpose, we first prepared a rod with the dimension 20 x 20 x 200 mm. The rod has then been rounded and polished to make a cylindrical preform (dimension  $\phi 17.8$  x 200 mm). The fabricated optical fiber is composed of a glass core made of SPCG4C while the cladding is made of polyacrylates with a lower refractive index (1.54). The drawing parameters were set as follows:

feeding speed 0.24 mm/min, drawing speed 4 – 6 m/min, temperature 540 – 550°C. Fibers with core diameter  $d = 125 \mu\text{m}$  and  $150 \mu\text{m}$  have been drawn successfully, the overall fiber diameter with the cladding was respectively  $225 \mu\text{m}$  and  $250 \mu\text{m}$  respectively (Fig. 10). We have experimentally proved that this glass could be used as waveguide for future development of optical fibers.

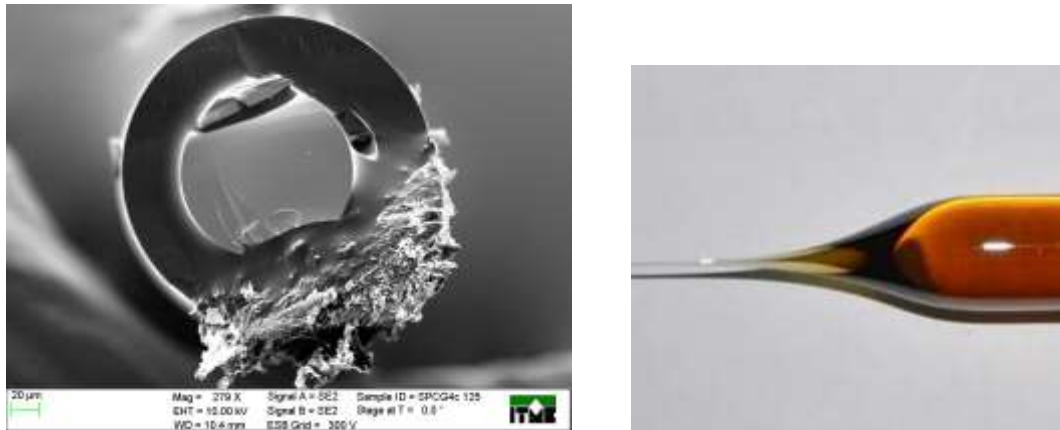


Figure 10 (Left) SEM photo of the fiber made of  $125 \mu\text{m}$  SPCG4C glass core and the polyacrylate cladding. (Right) end of preform of the glass core used to develop the fiber.

## Conclusions

The  $\text{SiO}_2\text{-PbO-CdO-Ga}_2\text{O}_3$  oxides system has been studied for the first time as a candidate for crystallization resistant glass for multiple thermal processing. Increasing the gallium oxide content instead of silica tends to increase the thermal stability of the glass against devitrification (as well as increasing the refractive index and the transmission towards mid-infrared). We showed that this system is suitable for the production of optical elements such as lenses and optical fibers due to its high thermal stability. Glass with the composition  $28\text{SiO}_2\text{-45PbO-15CdO-12Ga}_2\text{O}_3$  has been selected to develop optical components for its high crystallization resistance and its capacity to be molded. The optimized glass has a transmission up to  $5 \mu\text{m}$  with a refractive index  $n_D = 1.992$ . The glass transition temperature  $T_g = 460.8 \text{ }^\circ\text{C}$  and the softening temperature  $T_{sp} = 550 \text{ }^\circ\text{C}$ , respectively. The thermal stability criterion  $\Delta T = 193 \text{ K}$ . We have successfully fabricated lens by the hot embossing technique with an average roughness comprised between  $40 \text{ nm}$  and  $90 \text{ nm}$ . As a proof of glass feasibility for fiber technology, plastic-clad glass fibers were drawn with diameters of  $225 \mu\text{m}$  and  $250 \mu\text{m}$  and a core diameter of  $125 \mu\text{m}$  and  $150 \mu\text{m}$ .

## Acknowledgement

This work was supported by European Training Network H2020-MSCA-ITN-2016 Grant No 722380, SUPUVIR: Supercontinuum broadband light sources covering UV to IR applications and by the project TEAM TECH/2016-1/1 operated within the Foundation for Polish Science Team Programme co-financed by the European Regional Development Fund under Smart Growth Operational Programme (SG OP), Priority Axis IV.

## References

- [1] D. Pysz, I. Kujawa, R. Stępień, M. Klimczak, A. Filipkowski, M. Franczyk, L. Kociszewski, J. Buźniak, K. Haraśny and R. Buczyński, "Stack and draw fabrication of soft glass microstructured fiber optics", *Bull. Pol. Acad. Sci. Tech. Sci.*, volume 62(4), pp. 667-682 (2014).
- [2] I. Kujawa, R. Kasztelanic, R. Stępień, M. Klimczak, J. Cimek, A.J. Waddie, M.R. Taghizadeh, R. Buczyński, "Optimization of hot embossing method for development of soft glass microcomponents for infrared optics", *Opt. Laser Technol.*, volume 55, pp. 11-17 (2014).
- [3] R. Kasztelanic, I. Kujawa, R. Stępień, P. Kluczynski, A. Kozłowska, R. Buczyński, "Low-cost soft-glass diffractive and refractive lenses for efficient mid-IR fiber coupling systems", *Infrared Phys. Technol.*, Volume 71, pp. 307-312 (2015).
- [4] E.T.J. Nibbering, M.A. Franco, B.S. Prade, G. Grillon, C. Le Blanc, A. Mysyrowicz, "Measurement of the nonlinear refractive index of transparent materials by spectral analysis after nonlinear propagation", *Opt. Commun.*, volume 119(5-6) pp. 479-484 (1995).
- [5] <http://www.schott.com>.
- [6] J. Cimek, R. Stępień, M. Klimczak, I. Zalewska, R. Buczyński, "Development of thermally stable glass from SiO<sub>2</sub>-Bi<sub>2</sub>O<sub>3</sub>-PbO-ZnO-BaO oxide system suitable for all-solid photonic crystal fibers", *Opt. Mater.*, volume 73, pp 277-283 (2017).
- [7] J. Cimek, N. Liaros, S. Couris, R. Stępień, M. Klimczak, and R. Buczyński, "Experimental investigation of the nonlinear refractive index of various soft glasses dedicated for development of nonlinear photonic crystal fibers", *Opt. Mater. Express*, volume 7, pp. 3471-3483 (2017).
- [8] F. Gan, "Optical properties of fluoride glasses: a review", *J. Non-Cryst. Solids.*, volume 184, pp. 9-20 (1995).
- [9] R.A.H. El-Mallawany, "Tellurite Glasses Handbook: Physical Properties and Data", CRC Press (2001).
- [10] J.L. Adam, X. Zhang (Eds.), "Chalcogenide Glasses: Preparation, Properties and Applications", Woodhead Publishing, Oxford, Cambridge, New Delhi (2014).
- [11] E. Desurvire, "Erbium-doped fibre amplifier", Patent US 5005175 (1991).
- [12] Y. Fujimoto, N. Nakatsuka, "Optical amplification in bismuth-doped silica glass", *Appl. Phys. Lett.*, volume 82, pp. 3325-3326 (2003).
- [13] T. Murata, T. Mouri, "Matrix effect on absorption and infrared fluorescence properties of Bi ions in oxide glasses", *J. Non-Cryst. Solids*, volume 353, pp. 2403-2407 (2007).
- [14] M. Mortier, P. Goldner, P. Feron, G.M. Stephan, H. Xu, Z. Cai, "New fluoride glasses for laser applications", *J. Non-Cryst. Solids*, volume 326-327, pp. 505-509 (2003).
- [15] Y. Tian, T. Wei, X. Jing, J. Zhang, S. Xu, "Enhanced 2.7- and 2.9- $\mu\text{m}$  emissions in Er<sup>3+</sup>/Ho<sup>3+</sup> doped fluoride glasses sensitized by Pr<sup>3+</sup> ions", *Mater. Res. Bull.*, volume 76, pp. 67-71 (2016).
- [16] X. Jiang, N.Y. Joly, M.A. Finger, F. Babić, G.K.L. Wong, J.C. Travers, P.St.J. Russell, "Deep-ultraviolet to mid-infrared supercontinuum generated in solid-core ZBLAN photonic crystal fibre", *Nat. Photonics*, volume 9(2), pp. 133–139 (2015).
- [17] L. Sojka, Z. Tang, H. Zhu, E. Bereś-Pawlik, D. Furniss, A. B. Seddon, T. M. Benson, S. Sujecki., "Study of mid-infrared laser action in chalcogenide rare earth doped glass with Dy<sup>3+</sup> Pr<sup>3+</sup> and Tb<sup>3+</sup>", *Opt. Mater. Exp.*, volume 2(11), pp. 1632-1640, (2012).
- [18] A. Zakery, S.R. Elliott, "Optical properties and applications of chalcogenide glasses: a review", *J. Non-Cryst. Solids*, volume 330, pp. 1-12 (2003).
- [19] X.H. Zhang, Y. Guimond, Y. Bellec, "Production of complex chalcogenide glass optics by molding for thermal imaging", *J. Non-Cryst. Solids*, volume 326–327, pp. 519-523 (2003).
- [20] F. Starecki, F. Charpentier, J.L. Doualan, L. Quétel, K. Michel, R. Chahal, J. Troles, B. Bureau, A. Braud, P. Camy, V. Moizan, V. Nazabal, "Mid-IR optical sensor for CO<sub>2</sub> detection based on fluorescence absorbance of Dy<sup>3+</sup>:Ga<sub>5</sub>Ge<sub>20</sub>Sb<sub>10</sub>S<sub>65</sub> fibers", *Sensors Actuat. B*, volume 207, pp. 518-525 (2015).

- [21] M.L. Anne, C. Le Lan, V. Monbet, C. Boussard-Plédel, M. Ropert, O. Sire, M. Pouchard, C. Jard, J. Lucas, J.L. Adam, P. Brissot, B. Bureau, O. Loréal, "Fiber evanescent wave spectroscopy using the mid-infrared provides useful fingerprints for metabolic profiling in humans", *J. Biomed. Opt.*, volume 14, pp. 054033 (2009).
- [22] P. Lucas, C. Boussard-Plédel, A. Wilhelm, S. Danto, X.H. Zhang, P. Houizot, S. Maurugeon, C. Conseil, B. Bureau, "The development of advanced optical fibers for long-wave infrared transmission", *Fibers*, volume 1, pp. 110-118 (2013).
- [23] S. Cui, C. Boussard-Plédel, J. Lucas, and B. Bureau, "Te-based glass fiber for far-infrared biochemical sensing up to 16  $\mu\text{m}$ ", *Opt. Express*, volume 22, pp. 21253-21262 (2014).
- [24] B. Saisudha, T. Mallur, A. Ashish, K. Panakkattu, "Compositional dependence of optical band gap and refractive index in lead and bismuth borate glasses", *Mater. Res. Bull.*, volume 68, pp. 27 (2015).
- [25] A. Marczewska, M. Środa, M. Nocuń, B. Sulikowski, "Lead-gallium glasses and glass-ceramics doped with  $\text{SiO}_2$  for near infrared transmittance", *Opt. Mater.*, volume 45, pp.121-130 (2015).
- [26] J.C. Lapp and W.H. Dumbaugh, "Gallium Oxide Glasses", *Key Engineering Materials*, volume 94-95, pp. 257-278, (1994).
- [27] W.H. Dumbaugh and J.C. Lapp, "Heavy-Metal Oxide Glasses", *J. Am. Ceram. Soc.*, volume 75, pp. 2315-2326 (1992).
- [28] J.E. Shelby, "Lead Gallate Glasses", *J. Am. Ceram. Soc.*, volume 71, pp. 254-256 (1988).
- [29] H. Fan, G. Wang, L. Hu, "The Thermal and Optical Properties of  $\text{Bi}_2\text{O}_3\text{-B}_2\text{O}_3\text{-Ga}_2\text{O}_3$  Glasses", *Conference on Lasers and Electro-Optics, Pacific Rim* (2009).
- [30] J.C. Lapp, W.H. Dumbaugh, "Gallium oxide glasses", *Key Eng. Mater.*, volume 94–95, pp. 254-278 (1994).
- [31] I.B. Kacem, L. Gautron, D. Coillot, D.R. Neuville, Structure and properties of lead silicate glasses and melts, *Chem. Geol.*, Volume 461, pp. 104-114 (2017).
- [32] J.E. Shelby, *Introduction to Glass Science and Technology*, 2nd ed. Royal Society of Chemistry (2005).
- [33] J. Cimek, R. Stępień, G. Stepniewski, B. Siwicki, P. Stafiej, M. Klimczak, D. Pysz, R. Buczyński, "High contrast glasses for all-solid fibers fabrication", *Opt. Mater.*, volume 62, pp. 159-163 (2016).
- [34] J.H. Welch, "A simple microscope attachment for observing high-temperature phenomena", *J. Sci. Instrum.*, volume 31(12), pp. 458-462 (1954).
- [35] J.H. Welch, "Improved microfurnace power supply", *J. Sci. Instrum.*, volume 38(10), pp. 402-403 (1961).
- [36] A Dietzel, *Glasstech. Ber.*, volume 22, pp. 41 (1968).
- [37] P. Hlubina, "White-light spectral interferometry with the uncompensated Michelson interferometer and the group refractive index dispersion in fused silica", *Opt. Commun.*, volume 193, pp. 1-7 (2001).
- [38] D.L. Pye, A. Montenero, I. Joseph, "Properties of Glass-Forming Melts", *CRC Press*, pp. 489 (2005).
- [39] H.M. Oo, H. Mohamed-Kamari, and W.M.D. Wan-Yusoff. "Optical Properties of Bismuth Tellurite Based Glass", *Int. J. Mol. Sci.*, volume 13, pp. 4623-4631 (2012).
- [40] Y.B. Saddeek, B. Yasser, H.A. Afifi, N.S. Abd El-Aal, "Interpretation of mechanical properties and structure of  $\text{TeO}_2\text{-Li}_2\text{O-B}_2\text{O}_3$  glasses.", *Phys. B*, volume 398, pp. 1–7(2007).
- [41] I. Kujawa, R. Kasztelanica, R. Stępień, M. Klimczak, J. Cimek, A.J. Waddie, M.R. Taghizadeh, R. Buczyński, "Optimization of hot embossing method for development of soft glass micro components for infrared optic", *Opt.Las. Technol.*, volume 55, pp. 11-17 (2014).
- [42] R. Kasztelanica, I. Kujawa, R. Stępień, K. Haraśny, D. Pysz, R. Buczyński, "Molding of soft glass refraction mini lens with hot embossing process for broadband infrared transmission systems", *Infrared Phys. Technol.*, volume 61, pp. 299-305 (2013).



Annex 1: Sellmeier coefficients

	Sellmeier coefficients					
	B1	B2	B3	C1	C2	C3
SPCG1B	2.2860004	0.2676274	0.3363165	0.0195302	0.0862373	58.4360
SPCG2B	2.2934904	0.3122492	0.0962427	0.0144952	0.0995960	34.5907
SPCG3B	2.2496469	0.4128865	1.8550755	0.0191284	0.0738834	207.1074
SPCG4B	2.2879307	0.3843901	4.0000000	0.0259877	0.0576978	295.0608
SPCG5B	2.2832089	0.4251855	2.0558794	0.0190812	0.0789427	250.0000
SPCG0C	2.2260472	0.4580070	0.1151607	0.0161229	0.0736734	21.4515
SPCG1C	2.2065901	0.4374321	0.1308677	0.0178881	0.0749653	24.0461
SPCG3C	2.0058902	0.6685237	0.2016625	0.0144459	0.0673399	34.2226
SPCG4C	2.1276564	0.5839574	1.5320049	0.0159745	0.0728240	214.3810
SPCG5C	2.5992090	0.1272097	2.4008329	0.0258130	0.1132925	270.5981
SPCG0D	2.1585834	0.3944738	0.2863098	0.0167787	0.0715992	41.2875
SPCG1D	2.0008162	0.5652997	2.4000215	0.0140470	0.0653053	297.4703
SPCG2D	2.3015259	0.2754106	1.0046092	0.0190429	0.0844385	135.9643
SPCG3D	2.3975935	0.2000000	0.2449257	0.0213246	0.0918612	36.9704
SPCG4D	2.4000000	0.2464867	0.0657511	0.0198281	0.0932517	17.3433
SPCG5D	2.0443259	0.6266668	0.5674441	0.0146371	0.0691784	79.8454